AMERICAN SOCIETY FOR MICROBIOLOGY | mBio®

RESEARCH ARTICLE

Cyclic Enterobacterial Common Antigen Maintains the Outer Membrane Permeability Barrier of *Escherichia coli* in a Manner Controlled by YhdP

Angela M. Mitchell,[a] Tharan Srikumar,[a] Thomas J. Silhavy[a]

[a]Department of Molecular Biology, Princeton University, Princeton, New Jersey, USA

ABSTRACT Gram-negative bacteria have an outer membrane (OM) impermeable to many toxic compounds that can be further strengthened during stress. In *Enterobacteriaceae*, the envelope contains enterobacterial common antigen (ECA), a carbohydrate-derived moiety conserved throughout *Enterobacteriaceae*, the function of which is poorly understood. Previously, we identified several genes in *Escherichia coli* K-12 responsible for an RpoS-dependent decrease in envelope permeability during carbon-limited stationary phase. For one of these, *yhdP*, a gene of unknown function, deletion causes high levels of both vancomycin and detergent sensitivity, independent of growth phase. We isolated spontaneous suppressor mutants of *yhdP* with loss-of-function mutations in the ECA biosynthesis operon. ECA biosynthesis gene deletions suppressed envelope permeability from *yhdP* deletion independently of envelope stress responses and interactions with other biosynthesis pathways, demonstrating suppression is caused directly by removing ECA. Furthermore, *yhdP* deletion changed cellular ECA levels and *yhdP* was found to co-occur phylogenetically with the ECA biosynthesis operon. Cells make three forms of ECA: ECA lipopolysaccharide (LPS), an ECA chain linked to LPS core; ECA phosphatidylglycerol, a surface-exposed ECA chain linked to phosphatidylglycerol; and cyclic ECA, a cyclized soluble ECA molecule found in the periplasm. We determined that the suppression of envelope permeability with *yhdP* deletion is caused specifically by the loss of cyclic ECA, despite lowered levels of this molecule found with *yhdP* deletion. Furthermore, removing cyclic ECA from wild-type cells also caused changes to OM permeability. Our data demonstrate cyclic ECA acts to maintain the OM permeability barrier in a manner controlled by YhdP.

IMPORTANCE Enterobacterial common antigen (ECA) is a surface antigen made by all members of *Enterobacteriaceae*, including many clinically relevant genera (e.g., *Escherichia*, *Klebsiella*, *Yersinia*). Although this surface-exposed molecule is conserved throughout *Enterobacteriaceae*, very few functions have been ascribed to it. Here, we have determined that the periplasmic form of ECA, cyclic ECA, plays a role in maintaining the outer membrane permeability barrier. This activity is controlled by a protein of unknown function, YhdP, and deletion of *yhdP* damages the OM permeability barrier in a cyclic ECA-dependent manner, allowing harmful molecules such as antibiotics into the cell. This role in maintenance of the envelope permeability barrier is the first time a phenotype has been described for cyclic ECA. As the Gram-negative envelope is generally impermeable to antibiotics, understanding the mechanisms through which the barrier is maintained and antibiotics are excluded may lead to improved antibiotic delivery.

KEYWORDS ECA, *Enterobacteriaceae*, *Escherichia coli*, YhdP, enterobacterial common antigen, outer membrane

Received 15 June 2018 **Accepted** 11 July 2018 **Published** 7 August 2018

Citation Mitchell AM, Srikumar T, Silhavy TJ. 2018. Cyclic enterobacterial common antigen maintains the outer membrane permeability barrier of *Escherichia coli* in a manner controlled by YhdP. mBio 9:e01321-18. https://doi.org/10.1128/mBio.01321-18.

Editor Scott J. Hultgren, Washington University School of Medicine

Address correspondence to Thomas J. Silhavy, tsilhavy@princeton.edu.

The cellular envelope of Gram-negative bacteria consists of an inner membrane (IM) surrounding the cytoplasm, an asymmetrical outer membrane (OM), and a thin layer of peptidoglycan found in the periplasm separating the two membranes (1). While the inner leaflet of the OM is composed of phospholipids, the outer leaflet is mainly composed of lipopolysaccharide (LPS). LPS possesses a number of negatively charged residues that are bridged by divalent cations to form a strong network of interactions between neighboring LPS molecules (2). Due to these interactions and the amphiphilic nature of LPS, the OM provides the cell a robust permeability barrier, resistant to both large and hydrophobic molecules (3). For this reason, the OM has proven an impediment for the design of new antibiotics to treat Gram-negative bacterial infections.

Enterobacterial common antigen (ECA) is an invariant carbohydrate-derived molecule that is present in the OM and periplasm of members of *Enterobacteriaceae* (4). Although ECA is restricted to one family of bacteria, four of the seven species identified by the World Health Organization as being of high concern due to frequent antibiotic-resistant infections are members of this family (*Klebsiella pneumoniae*, *Escherichia coli*, nontyphoidal *Salmonella*, and *Shigella* species) (5). Despite the conserved nature of this molecule within *Enterobacteriaceae* (6), its function is largely unknown. In part, this is because the biosynthesis pathways for ECA, O antigen, and peptidoglycan overlap in such a way that gene deletions preventing ECA biosynthesis often also prevent O-antigen production (7–9) or perturb peptidoglycan biosynthesis, causing envelope stress responses to be activated (i.e., Cpx, Rcs, σ^E) (10–12). Thus, in interpreting the results of high-throughput screens (13–16), it is difficult to determine whether phenotypes are directly related to the presence or absence of ECA or are instead related to changes to other aspects of the cell envelope. Nevertheless, it is thought that ECA plays a small role in bile salt resistance and in organic acid resistance (17, 18). It is generally assumed that the surface-exposed forms of ECA are responsible for these phenotypes. In addition, in *Salmonella enterica* serovar Typhimurium, O-antigen and ECA biosynthesis are not genetically connected, and the first gene in ECA biosynthesis, *wecA*, can be deleted without activating stress responses, affecting O-antigen biosynthesis, or impairing peptidoglycan biosynthesis (19). Studies in this strain have demonstrated that cells without ECA are deficient in pathogenesis (19), suggesting that ECA plays an important role in the host.

The structure of ECA is conserved throughout *Enterobacteriaceae*, with each unit of ECA consisting of GlcNAc (*N*-acetylglucosamine), ManNAcA (*N*-acetyl-D-mannosaminuronic acid), and Fuc4NAc (4-acetamido-4,6-dideoxy-D-galactose) (20, 21). The pathway of ECA biosynthesis is analogous to that of O-antigen biosynthesis (see Fig. S1 in the supplemental material). GlcNAc-1-phosphate is linked to undecaprenyl-phosphate (Und-P), a lipid carrier in the IM also used for the biosynthesis of O antigen, peptidoglycan, and capsule carbohydrates, and then ManNAcA and Fuc4NAc are attached (22, 23). Many genes in the ECA biosynthesis operon are responsible for synthesizing these sugars and linking them to Und-P (22, 24, 25). The ECA unit linked to Und-P is then flipped across the IM by WzxE (26). The ECA chains are polymerized by WzyE (27), and the chain length is controlled by WzzE (28). Three forms of ECA are made from polymerized ECA chains. In the first, LPS-linked ECA (ECA_{LPS}), the ECA chain is transferred to the core sugar moiety of LPS by WaaL (29), the same gene responsible for attaching O antigen to core, and the molecule is transferred to the cell surface, presumably by the Lpt system. In the second, phosphatidylglycerol-linked ECA (ECA_{PG}), the ECA chain is attached to phosphoglyceride by a phosphodiester linkage (30) and the molecule is surface exposed through an unknown pathway (31, 32). In the third form, cyclic ECA (ECA_{CYC}), an ECA chain of a precise chain length (4 to 6, depending on species) is cyclized in a reaction dependent on WzzE (33–35). This molecule remains in the periplasm (34).

Previously, we investigated changes to the *Escherichia coli* K-12 OM that occur during growth under different nutrient conditions (36) and determined that an RpoS-dependent mechanism strengthens the envelope permeability barrier under carbon-limiting conditions in a manner that depends on the presence of the genes for several proteins. Of these, YhdP is a large protein of unknown function that is predicted to be

located in the IM with the majority of the protein exposed to the periplasm (37). Unlike our other hits, *yhdP* deletion (Δ*yhdP*) has strong phenotypes regardless of growth phase. In fact, in a large-scale study on the effects of gene deletions on chemical sensitivity (38), *yhdP* scored second highest for SDS EDTA (sodium dodecyl sulfate, ethylenediaminetetraacetic acid) sensitivity as well as in the top 15 hits for vancomycin sensitivity. Despite the high level of envelope permeability caused with deletion of *yhdP*, the function of YhdP is completely unknown. In addition, *yhdP* appears to be restricted phylogenetically (39), suggesting that it may play a role that is specific to a subset of species.

Here, we demonstrate that mutations that block ECA biosynthesis restore the envelope permeability barrier of Δ*yhdP* strains. Furthermore, we demonstrate that *yhdP*, which phylogenetically co-occurs with ECA biosynthesis genes, directly or indirectly controls ECA levels. We were able to trace the suppression specifically to the removal of ECA_{CYC} and demonstrate that, even in a wild-type background, removing ECA_{CYC} changes the OM permeability barrier. Therefore, ECA_{CYC} plays a role in maintaining the OM permeability barrier, and its activity is regulated by YhdP.

RESULTS

Deletion of *yhdP* causes OM permeability. Our initial screen identifying *yhdP* was based on sensitivity to SDS treatment during stationary phase, and we also found that Δ*yhdP* caused sensitivity to 2% SDS in actively growing cells (36); therefore, we treated *yhdP*$^+$ and Δ*yhdP* cells with SDS and increasing concentrations of EDTA and measured their growth. EDTA disrupts the bridging of LPS molecules by divalent cations, sensitizing the OM to the presence of detergents and allowing for the detection OM defects (40). Both *yhdP*$^+$ and Δ*yhdP* cells grew to stationary phase with 0.05% SDS alone; however, a low concentration of EDTA (0.25 mM) caused a large growth defect in Δ*yhdP* cells, while causing a minimal effect on *yhdP*$^+$ cells (Fig. 1A). In addition, a higher concentration of EDTA (0.5 mM) completely impaired the growth of Δ*yhdP* cells, while still allowing for growth of *yhdP*$^+$ cells. These data suggest that there is a change in outer membrane structure when YhdP is removed, and so we investigated whether Δ*yhdP* causes permeability to other toxic agents.

Disk assay results suggested that Δ*yhdP* cells might be sensitive to vancomycin. Vancomycin is a glycopeptide antibiotic that targets peptidoglycan biosynthesis, which is commonly used to treat antibiotic-resistant Gram-positive infections but is largely incapable of traversing the Gram-negative OM (41). Permeability of the OM to vancomycin is thought to be caused by "cracks" between patches of phospholipids and LPS (42). We analyzed growth curves of *yhdP*$^+$ and Δ*yhdP* cells with increasing dosages of vancomycin. Similarly to Δ*yhdP*'s SDS EDTA sensitivity, a low dose of vancomycin (50 μg/ml) caused lysis of Δ*yhdP* cells while not affecting *yhdP*$^+$ growth (Fig. 1B). A higher dose of vancomycin (100 μg/ml) completely inhibited growth of Δ*yhdP* cells while only minimally affecting *yhdP*$^+$ cells. In fact, the increase in vancomycin sensitivity with Δ*yhdP* can also be observed by a lowering of the vancomycin MIC (MIC) for this strain (Fig. S2). Both the increased vancomycin and SDS EDTA sensitivity of Δ*yhdP* cells suggest that there is a change in OM structure in this mutant that leads to increased permeability.

Disrupting ECA biosynthesis suppresses envelope permeability in Δ*yhdP* strains. As no functions are known for YhdP, we then sought to isolate mutations suppressing strain Δ*yhdP*'s envelope permeability defects in order to determine in what pathway YhdP might be working. The slight growth we observed late after SDS EDTA and vancomycin treatment (Fig. 1) suggested that spontaneous suppressor mutants are common within Δ*yhdP* strain cultures. Therefore, we plated Δ*yhdP* cells on a concentration of vancomycin at which growth of these cells is inhibited but *yhdP*$^+$ cells could grow, and we isolated spontaneous suppressor mutants that were capable of growth on this medium. Then, we conducted a secondary screen of these suppressors to identify those that restored both vancomycin and SDS EDTA resistance. We isolated seven spontaneous suppressors that restored both phenotypes, all of which mapped to

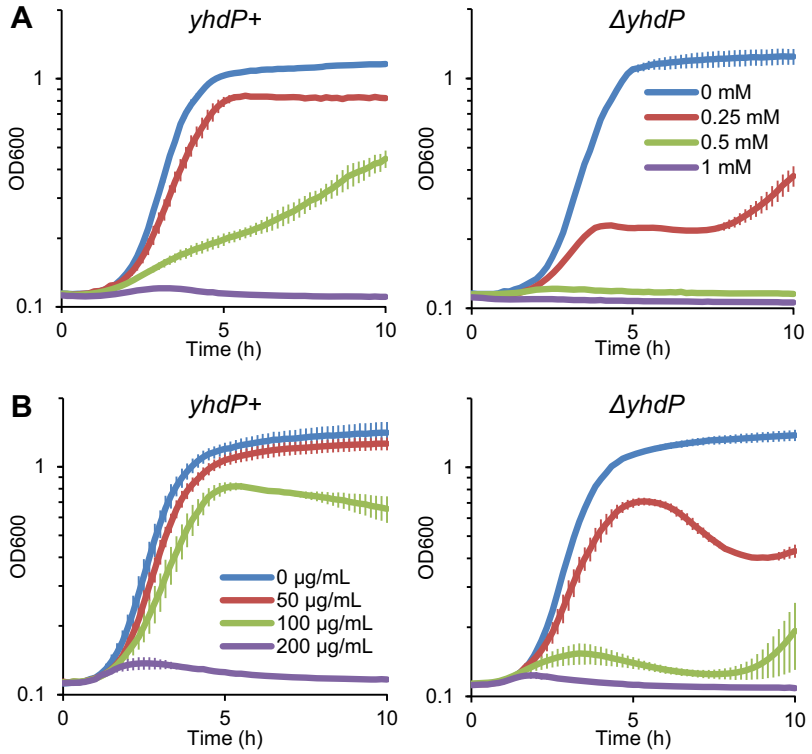

FIG 1 Deletion of *yhdP* causes SDS EDTA and vancomycin sensitivity. (A) Cells with wild-type *yhdP* or from a Δ*yhdP* deletion mutant were diluted into fresh media containing 0.05% SDS and the indicated concentration of EDTA, and growth was assayed based on the OD_{600} every 10 min. The Δ*yhdP* strain was more sensitive to EDTA in the presence of SDS than the *yhdP*$^+$ strain. (B) Cells were grown as described for panel A, with the indicated concentration of vancomycin. The Δ*yhdP* strain lysed at lower concentrations of vancomycin than those that affected the *yhdP*$^+$ strain. Data are averages of three independent biological replicates ± the SEM on a $\log_{10}$ scale.

the ECA biosynthesis (*wec*) operon. All seven appeared to be loss-of-function alleles (Fig. 2A and B).

We then asked whether suppression of the Δ*yhdP* strain envelope permeability by disruption of the *wec* operon is specific to *yhdP* or is a general mechanism of vancomycin and SDS EDTA resistance. To answer this question, we utilized a deletion allele of *bamE*, a component of the β-barrel assembly machine responsible for folding outer membrane proteins (OMPs) into the outer membrane (43). Removal of this nonessential lipoprotein from the complex leads to a similar level of vancomycin sensitivity as Δ*yhdP* and causes slight SDS EDTA sensitivity (44, 45). We combined this deletion with a deletion of *wecA*, which is responsible for the addition of the first sugar in ECA to Und-P (46). Some vancomycin resistance was caused by deletion of *wecA* alone (Fig. 2C). When combined with a deletion of *bamE*, *wecA* deletion caused only minimal suppression of vancomycin sensitivity and worsened the *bamE* SDS EDTA sensitivity. In contrast, *wecA* deletion fully suppressed both the vancomycin and SDS EDTA sensitivities of a Δ*yhdP* strain. These data demonstrate that disruption of ECA biosynthesis is not a universal suppressor of vancomycin and SDS EDTA sensitivity and suggest that this suppression is specific to the Δ*yhdP* strain.

We conducted a transposon mutagenesis screen in an effort to identify additional suppressors of the Δ*yhdP* mutant strain envelope permeability. Briefly, we identified vancomycin-resistant clones from a pool of 10,000 transposon mutants in a Δ*yhdP* strain, mapped the transposon insertion sites in these mutants, and conducted a secondary screen for SDS EDTA resistance (Fig. S3A). The only mutations we identified that suppressed both the vancomycin and SDS EDTA phenotypes were in the *wec* operon (Table S1); furthermore, we identified mutations in every gene in the *wec*

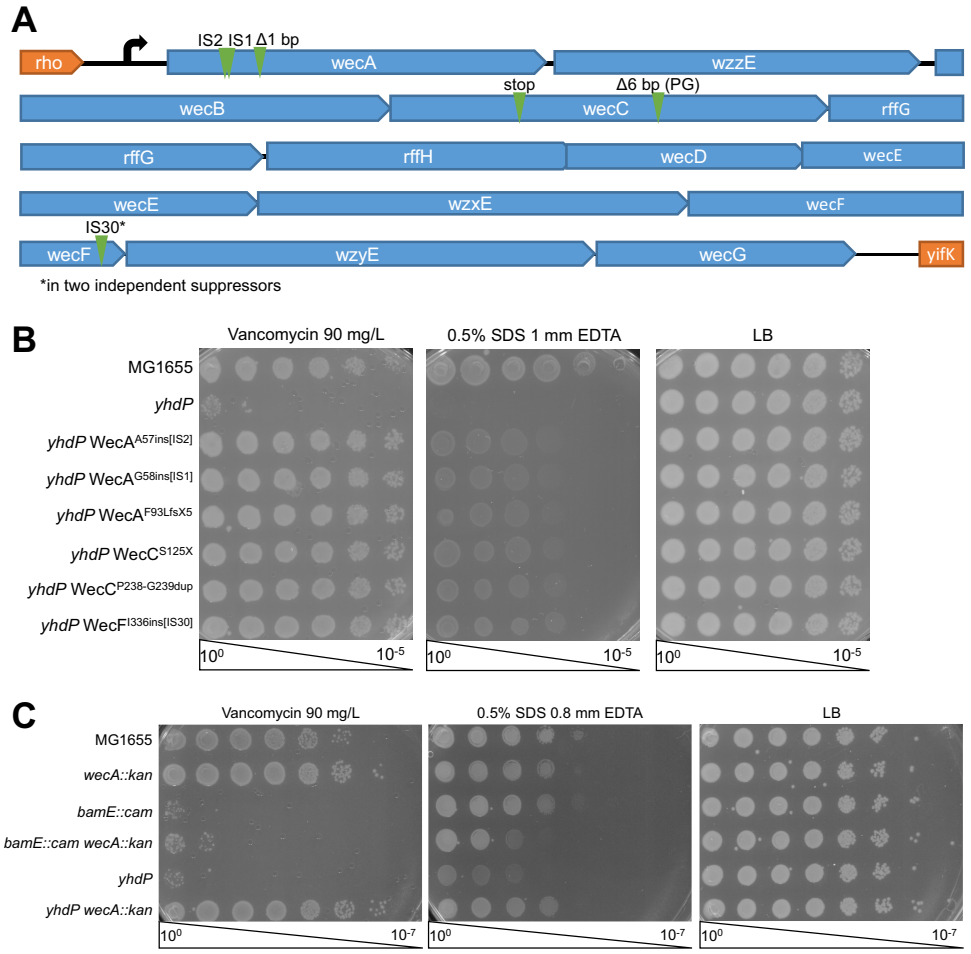

FIG 2 Loss-of-function mutations in ECA biosynthesis suppress Δ*yhdP*. Screening for suppressors of Δ*yhdP* vancomycin and SDS EDTA sensitivity led to the isolated seven suppressor mutations. (A) The locations of the suppressing mutations, all of which map to the *wec* operon, are shown. IS, native insertion sequence. (B) Efficiency of plating assays (EOPs) were performed by plating serial dilutions of the indicated culture on LB plates with the indicated additions to gauge to what degree the suppressor mutants suppressed the Δ*yhdP* strain's phenotypes. Complete suppression of vancomycin sensitivity and almost complete suppression of SDS EDTA sensitivity were observed. (C) EOPs were performed to determine whether suppression of vancomycin and SDS EDTA sensitivity by loss-of-function mutations in the *wec* operon was universal. Deletion of *wecA* suppressed the Δ*yhdP* strain but not deletion of *bamE*, suggesting the suppression is specific to *yhdP*. EOP images are representative of three independent experiments.

operon except those that are redundant with O-antigen biosynthesis genes (*rffG*, *wzxE*) (34, 47) and *wzyE*, for which disruption is toxic (34) (Fig. S3B). Given that the *wec* genes form an operon, it is likely that some of these insertions may be polar. With more than 2× genome coverage, *wec* operon mutations were the only mutations to suppress both of Δ*yhdP*'s phenotypes, suggesting that our suppressor screen may be saturated.

Loss of ECA is directly responsible for the suppression of the Δ*yhdP* strain. Because the ECA biosynthetic pathway interacts with the biosynthesis pathway for peptidoglycan and other extracytoplasmic glycans, disruption of ECA biosynthesis can cause cellular changes that are more wide-ranging than simple removal of ECA. Specifically, O-antigen biosynthesis, peptidoglycan biosynthesis, and ECA biosynthesis all compete for both precursor sugar molecules and for the lipid carrier on which the molecules are assembled, Und-P. Although our strains are O-antigen negative, when intermediate steps in the ECA biosynthesis pathway are disrupted, ECA intermediates (aminoglycans linked to Und-P-P) accumulate and sequester Und-P, stressing the peptidoglycan biosynthesis pathway (10). In contrast, when the first step in ECA biosynthesis (catalyzed by WecA) (46) is prevented, the pool of sugar precursors and

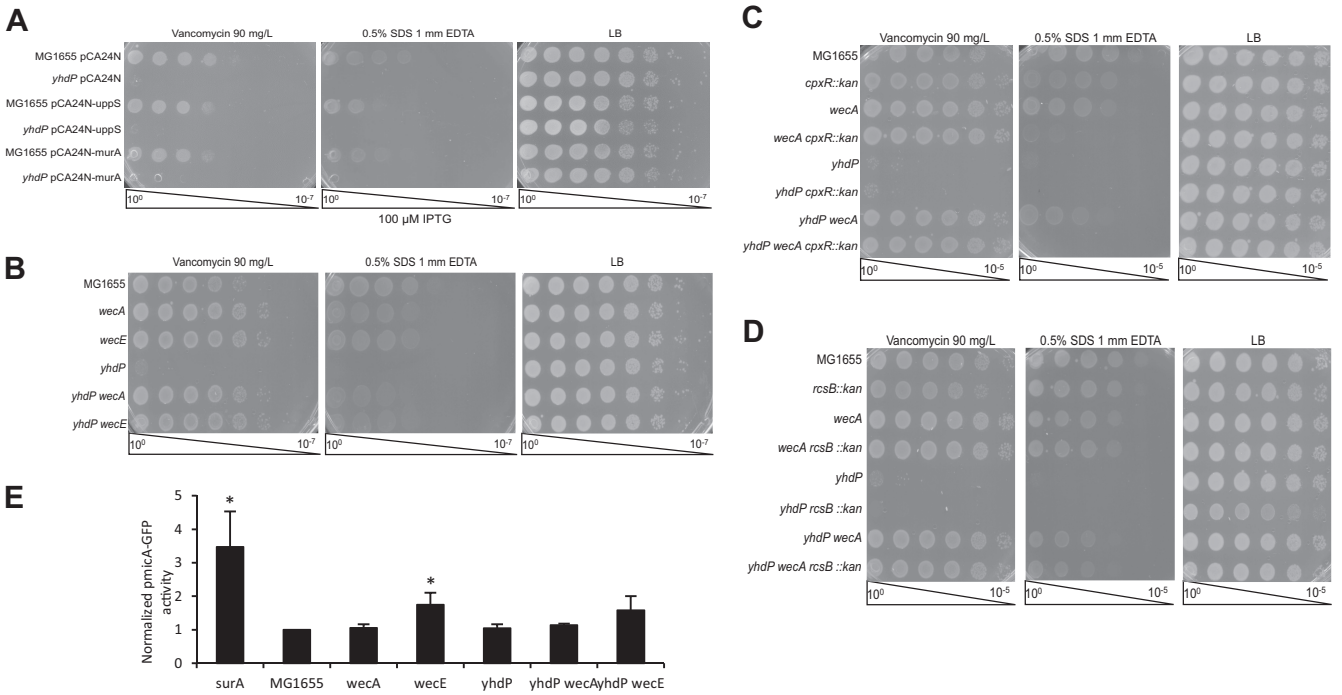

FIG 3 Suppression does not relate to Und-P availability or stress responses. (A) To determine whether the Δ*yhdP* strain is suppressed by relieving Und-P stress, EOPs were performed on strains carrying the indicated overexpression constructs. Overexpression of *uppS* and *murA* did not suppress the Δ*yhdP* strain, demonstrating that the Δ*yhdP* strain's phenotypes are not caused by effects of Und-P stress on peptidoglycan. (B) EOPs were performed to determine whether disruptions in ECA biosynthesis that increased Und-P availability for peptidoglycan synthesis (Δ*wecA*) and that decreased Und-P availability for peptidoglycan synthesis (Δ*wecE*) both suppress the Δ*yhdP* strain phenotypes. Both of these mutations suppressed the Δ*yhdP* strain phenotypes to an equal extent, suggesting that suppression is unrelated to Und-P availability. (C) EOPs were performed to determine whether the Cpx response was responsible for suppression of the Δ*yhdP* strain's phenotypes by disruptions of ECA biosynthesis. Suppression was observed with *wecA* deletion, even in the presence of *cpxR* deletion, demonstrating that the Cpx response is not necessary for suppression. (D) EOPs were performed to determine whether the Rcs response was required for suppression. Suppression was observed in the presence of *rcsB* deletion, demonstrating that the Rcs response is not necessary for the suppression of the Δ*yhdP* strain's phenotypes. EOPs images are representative of three independent experiments. (E) Activity of a σ^E reporter was assayed to determine whether suppression of the Δ*yhdP* strain correlated with σ^E activation. Suppression of the Δ*yhdP* strain's phenotypes did not correlate with σ^E activation, suggesting this is not the mechanism of suppression. Data shown are the average results of three independent biological replicates ± the SEM. Significance was calculated using the Mann-Whitney test. *, $P < 0.05$ compared to the appropriate parent strain (MG1655 or Δ*yhdP*).

Und-P available for peptidoglycan synthesis is increased. Therefore, we sought to determine whether (i) the phenotypes of Δ*yhdP* mutant cells were caused by Und-P stress and (ii) whether relieving Und-P stress suppresses the Δ*yhdP* strain.

Stress on the pool of Und-P has previously been detected using linkage disruption with a marker linked to *mrcB*::*kan* (48). As *mrcB* (PBP1B) is important for transglycosylation and transpeptidation of peptidoglycan precursors (49), deletion of *mrcB* in a strain with stress on the pool of available Und-P causes significant toxicity and can be synthetically lethal. This causes disruption of the linkage between the Tn*10* marker and the *mrcB* deletion (i.e., fewer colonies with the Tn*10* marker have received the *mrcB* deletion). However, we detected no linkage disruption with the Δ*yhdP* strain in the presence or absence of *wecA* (Fig. S4A), suggesting that the Δ*yhdP* mutant does not cause lipid carrier stress. To relieve possible Und-P stress, we overexpressed *uppS*, responsible for synthesizing Und-P, and *murA*, responsible for the first committed step in peptidoglycan synthesis (50, 51). Overexpression of these genes has previously been shown to relieve peptidoglycan stress caused by Und-P availability (48, 52). Overexpression of these genes had no effect on envelope permeability in a Δ*yhdP* background (Fig. 3A). Overexpression of *uppP*, a gene responsible for recycling Und-P (53), and *mrcB*, the gene encoding PBP1B, also had no effect on the Δ*yhdP* strain's envelope permeability (Fig. S4B). These data show that the phenotypes of the Δ*yhdP* deletion mutant are not caused by Und-P stress.

To verify further that the mechanism of Δ*yhdP* strain suppression by disruption of the ECA biosynthesis operon was not through effects on Und-P, we asked whether

deletion of the first gene in ECA synthesis, *wecA*, and deletion of a gene in an intermediate step of ECA synthesis, *wecE*, would have to the same effects on envelope permeability in a Δ*yhdP* strain. Deletions of both *wecA* and *wecE* caused slight vancomycin resistance and SDS EDTA sensitivity in a *yhdP*$^+$ background; however, when they were combined in the Δ*yhdP* deletion strain, the vancomycin and SDS EDTA resistance were both restored to the level of the ECA mutants alone (Fig. 3B). As both Δ*wecA* and Δ*wecE* mutant strains fully suppress the envelope permeability defects of a Δ*yhdP* strain despite having opposite effects on availability of Und-P and precursors, these data demonstrate that the suppression for the Δ*yhdP* strain is not due to modification of the peptidoglycan biosynthesis pathway.

Because of peptidoglycan defects and the accumulation of Und-P-linked ECA precursors, disruption of the ECA operon can also activate the Cpx, Rcs, and σ^E stress responses (10, 11). In fact, in *Serratia marcescens*, even disruption of *wecA* can activate the Rcs response (12). Therefore, we tested whether activation of stress responses was responsible for suppression of the Δ*yhdP* strain's envelope permeability by disruption of the ECA biosynthesis operon. The Cpx and Rcs stress responses are nonessential and their activity can be prevented by removal of their response regulators, CpxR and RcsB, respectively (54, 55). Disruption of *cpxR* has no effect on the suppression of the Δ*yhdP* strain's vancomycin sensitivity by Δ*wecA*, although synthetic SDS EDTA sensitivity in Δ*wecA* Δ*cpxR* double mutants prevents assessment of the role of Cpx on SDS EDTA sensitivity caused by *yhdP* deletion (Fig. 3C). Disruption of *rcsB* has no effect on the suppression of either the Δ*yhdP* strain's vancomycin or SDS EDTA sensitivity by the *wecA* deletion (Fig. 3D). These data demonstrate that neither the Cpx nor the Rcs stress response is necessary for the suppression of the Δ*yhdP* strain's phenotypes by the disruption of ECA biosynthesis. Although the σ^E response is essential in *E. coli* (56), the activation of the σ^E response can be monitored using reporters linked to σ^E-responsive promoters. One such reporter consists of the *micA* promoter, driving expression of green fluorescent protein (GFP) (57). Using this reporter, we found that activation of the σ^E response by ECA operon disruptions was not necessary for these disruptions to suppress the Δ*yhdP* strain's envelope permeability (Fig. 3E). These data together with the rarity of other suppressing mutations for Δ*yhdP* strongly suggest that YhdP is functionally connected with ECA.

The genes for YhdP and ECA occur in the same genomes. As our data suggested that ECA and YhdP may interact and ECA is restricted to *Enterobacteriaceae*, we examined the phylogenetic distribution of *yhdP*. We used STRING-DB (39) to search for possible homologues of *yhdP* and to score the homology of the detected genes. The vast majority of the homologues for *yhdP* were found to be in *Enterobacteriaceae*. In fact, homologues of YhdP outside of *Enterobacteriaceae* are only detected in some other Gammaprotobacteria and some Betaprotobacteria; however, none of the YhdP homologues detected for YhdP outside of *Enterobacteriaceae* had a higher homology with *E. coli* K-12 YhdP than a possible homologue in Indian rice (*Oryza sativa* Indica) (Fig. S5A). As YhdP is part of a family of proteins, the AsmA family (58), the *yhdP* homologues detected outside *Enterobacteriaceae* possibly represent other members of the AsmA family.

To examine further the distribution of the ECA biosynthetic genes and *yhdP*, we used STRING-DB (39) to calculate phylogenetic co-occurrence scores based on genes with homology found across genomes. The three genes within the *wec* operon whose products form a complex to flip ECA to the outer leaflet of the IM (*wzxE*), polymerize ECA (*wzyE*), and control ECA chain length (*wzzE*) have phylogenetic co-occurrence scores with each other of 0.70 to 0.78 (Fig. S5B). The co-occurrence scores for these genes with *yhdP* range from 0.40 to 0.76, which are within the range of the co-occurrence scores for pairs of genes within the *wec* operon (0.15 to 0.78). The highest co-occurrence pair for *yhdP* was found with *wzzE*. These data demonstrate that genomes containing the machinery to make ECA also contain *yhdP*.

YhdP changes ECA levels. Given that YhdP and ECA are functionally related, we investigated whether deletion of Δ*yhdP* causes changes to ECA abundance or chain length. There is no apparent change in the surface exposure of ECA_{PG} or ECA_{LPS} in the absence of *yhdP* (Fig. S6). By immunoblotting, we detected ECA_{LPS} and ECA_{PG} and compared the levels and chain length with and without *yhdP* (Fig. 4B). We observed a range of bands with the lowest molecular weight band likely indicating molecules with one repeat unit of ECA and higher molecular weight bands indicating molecules with more repeat units of ECA. Lanes 2 and 7 show a combination of ECA_{LPS} and ECA_{PG} due to the wild-type genetic background, while lanes 4 and 9 (Δ*waaL* strains) show ECA_{PG} alone, as ECA_{LPS} cannot be produced in these strains (Fig. 4A). Given the lack of bands with Δ*wecA* samples where there is no ECA, all bands other than the band designated with an asterisk were taken to be ECA. Due to the use of a polyclonal antibody, the levels of ECA_{LPS} and ECA_{PG} cannot be directly compared.

There was no apparent difference in chain length between *yhdP*$^+$ and Δ*yhdP* strains (lanes 2 and 7); however, levels of ECA_{LPS} and ECA_{PG} together (lanes 2 and 7) were higher in a Δ*yhdP* strain than in a *yhdP*$^+$ strain. This is also true for ECA_{PG} alone (lanes 4 and 9). Interestingly, this 2- to 3-fold increase in ECA levels only occurred in the presence of *wzzE* (Fig. 4C). The reason for the large increase in ECA_{PG} levels between the Δ*waaL* and Δ*wzzE* Δ*waaL* strains remains an interesting question for further investigation.

Unlike the lipid-linked forms of ECA, ECA_{CYC} is not charged and cannot be detected by immunoblotting (Fig. 4A). Instead, we utilized a quantitative MALDI-TOF (matrix-assisted laser desorption ionization-time of flight) approach to detect and quantitate ECA_{CYC} in purified samples. By examining the *m/z* ratios of ECA_{CYC} peaks, which are present in *wzzE*$^+$ strains and absent in Δ*wzzE* strains (Fig. 4A), we determined that the cyclization and nonstoichiometric acetylation of ECA_{CYC} were not changed in a Δ*yhdP* strain (Fig. S7A). Therefore, to quantitate ECA_{CYC} levels, we utilized Δ*wecH* strains that do not acetylate ECA and that do not affect Δ*yhdP* phenotypes to minimize the number of ECA_{CYC} peaks. We then grew *yhdP*$^+$ strains with a nitrogen source containing ^{15}N and Δ*yhdP* cells with a nitrogen source containing ^{14}N. This shifted the *m/z* ratio of the ECA_{CYC} by 12, as ECA_{CYC} contains 12 nitrogen atoms, and allowed the comparison of the *yhdP*$^+$ and Δ*yhdP* strains' ECA_{CYC} on the same spectra (Fig. S7B).

To quantitate relative ECA_{CYC} levels, we combined *yhdP*$^+$ cells grown with ^{15}N with an equal number of Δ*yhdP* cells grown with ^{14}N as one sample before purification of ECA_{CYC}, allowing direct comparison of the peaks generated from each strain. This approach indicated that levels of ECA_{CYC} are decreased in the Δ*yhdP* strain (Fig. 4D). Over several biological replicates, we found the decrease in the Δ*yhdP* strain to be almost 8-fold (Fig. 4E). The phylogenetic co-occurrence of *yhdP* with ECA biosynthesis genes and the changes to ECA in the absence of YhdP provides further evidence that YhdP plays a role related to ECA.

YhdP prevents ECA_{CYC} from damaging the OM permeability barrier. Given that the different forms of ECA are present in different cellular compartments and presumably play different roles, we then asked which form of ECA is responsible for the Δ*yhdP* strain's phenotypes. We hypothesized that one of the membrane-associated forms of ECA would be responsible for the permeability defects, as these molecules are part of the OM and the levels of these molecules are increased when YhdP is removed. We tested this hypothesis by removing specific forms of ECA and determining whether the Δ*yhdP* strain's envelope permeability was suppressed.

We compared *wecA* deletion, which removes all forms of ECA (46) and suppresses, with *waaL* deletion, which specifically prevents the formation of ECA_{LPS} (29), and with *wzzE* deletion, which prevents the formation of ECA_{CYC} but allows the formation of ECA_{LPS} and ECA_{PG}, albeit with random chain length (28, 34). Currently, there is no way to remove ECA_{PG} without removing the other forms of ECA. We observed full suppression of the Δ*yhdP* strain's envelope permeability with both the *wecA* and *wzzE* deletions; however, *waaL* deletion had no effect on the Δ*yhdP* strain's phenotypes (Fig. 5A).

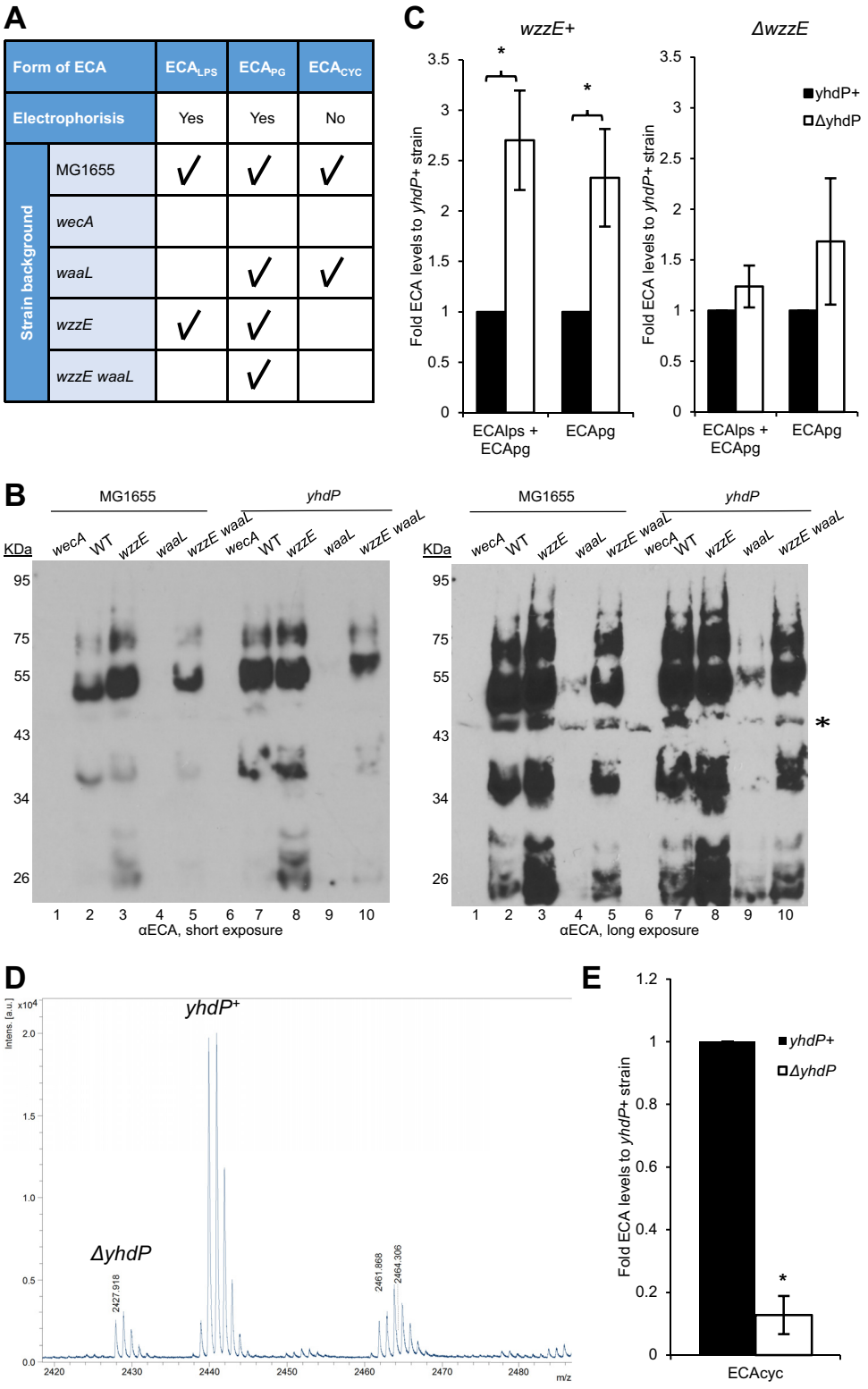

FIG 4 YhdP interacts genetically with ECA. (A) Distinctions between forms of ECA are shown in table form, including whether they can be subjected to PAGE analysis and immunoblotting ("electrophoresis") and which forms are present in genetic backgrounds with the indicated gene deletions. The presence of the form of ECA is indicated with a check mark. (B) Immunoblot analysis was performed for strains with the indicated gene deletions and probed with anti-ECA antibody to assay changes to ECA caused by the *yhdP* deletion. Strains with no mutations other than *yhdP*$^{+/-}$ are indicated by WT. Bands from low molecular weights to high molecular weights represent increasing ECA chain lengths. The types of ECA that can be observed in each genetic background are detailed in Fig. 4A. Short and long exposures are shown. *, a nonspecific band. All other bands are forms of ECA.

(Continued on next page)

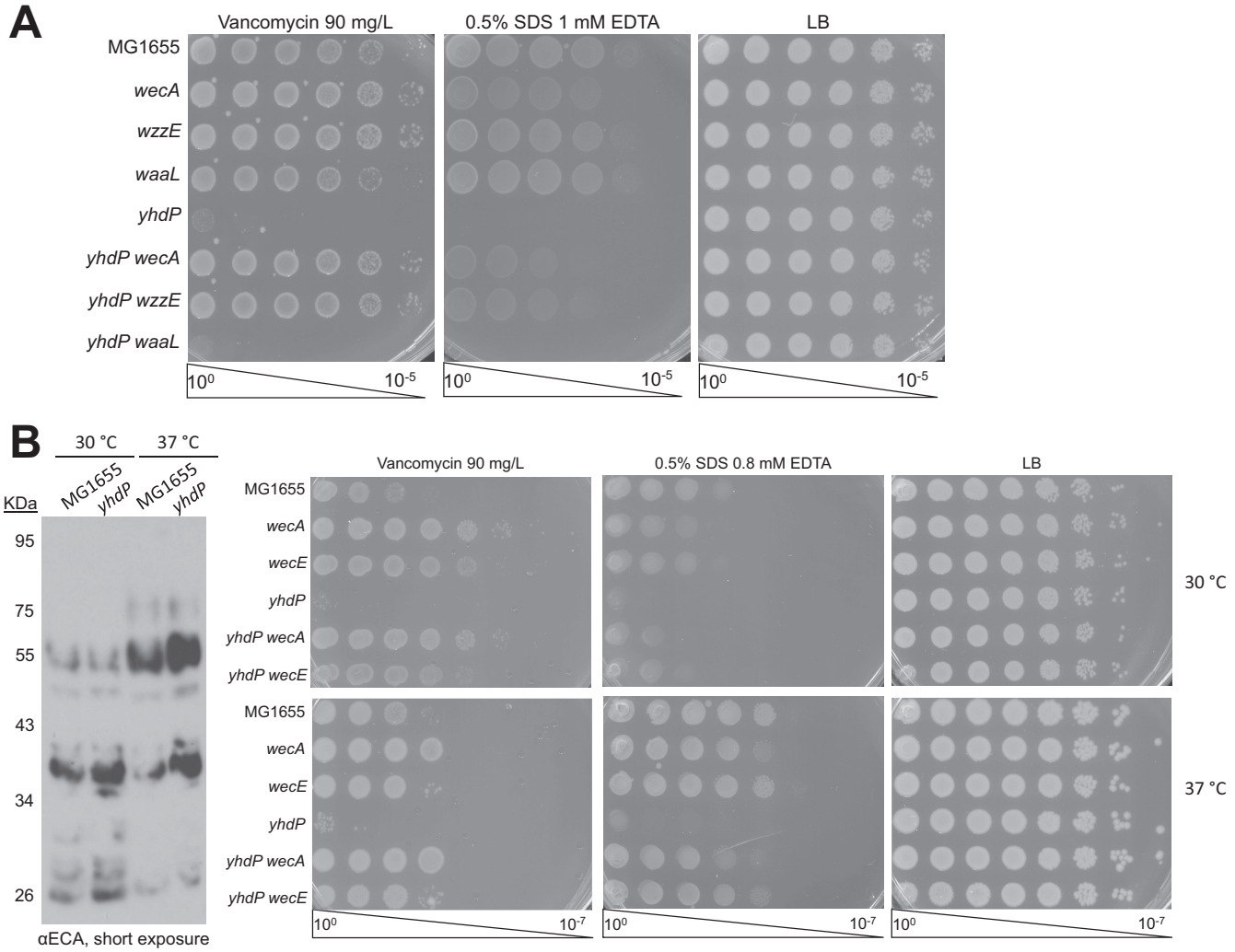

FIG 5 Antibiotic sensitivity from the Δ*yhdP* strain is mediated by a functional interaction with ECA_{CYC}. (A) To determine what form of ECA is important for causing the Δ*yhdP* strain's phenotypes, EOPs were performed on strains with the indicated deletions. Suppression by *wzzE* deletion and lack of suppression by *waaL* deletion suggest that ECA_{CYC} may be responsible for the Δ*yhdP* strain's phenotypes. (B) To eliminate the possibility that suppression in a Δ*wzzE* deletion strain occurs through changes in ECA chain length, EOPs were performed at 30°C and at 37°C to assay the Δ*yhdP* strain's phenotypes. Immunoblot analysis was used to determine ECA chain length at these temperatures. The model chain length of ECA was found to be four at 30°C and six at 37°C. However, the Δ*yhdP* strain has strong phenotypes at both temperatures, suggesting that changes in chain length are not responsible for suppression. All images are representative of three independent experiments.

These data demonstrate that ECA_{LPS} does not contribute to the Δ*yhdP* strain's phenotypes. The suppression of the Δ*yhdP* strain by *wzzE* deletion did not rely on stress response activation (Fig. S8).

WzzE is the chain length regulator for ECA (28) and its removal causes several changes to ECA, some of which can be observed in Fig. 4B (compare lanes 2 and 3 and

FIG 4 Legend (Continued)
Images are representative of five independent experiments. (C) Densitometry was performed from immunoblots to quantitate levels of the indicated types of ECA in the given background. The levels of membrane-bound ECA were found to be higher with the Δ*yhdP* strain only when *wzzE* was present. Fold values compared to the *yhdP*$^+$ strain are shown as the average of three to five independent experiments ± the SEM. (D) Levels of ECA_{CYC} were analyzed by MALDI-TOF with relative values comparing *yhdP*$^+$ cells labeled with ^{15}N to Δ*yhdP* cells. Cells were combined before purification to allow for direct comparison of levels of heavy ECA_{CYC} (*m/z* 2,440) and normal ECA_{CYC} (*m/z* 2,428). A representative image is shown and normal and heavy peaks are labeled by their originating strain. The unlabeled higher-molecular-weight species is a modified form of ECA_{CYC}. (E) Quantification of ECA_{CYC} levels is shown as average relative levels from three biological replicates ± the SEM. Levels of ECA_{CYC} were lowered in a strain Δ*yhdP* background. *, $P < 0.05$ compared to the *yhdP*$^+$ strain.

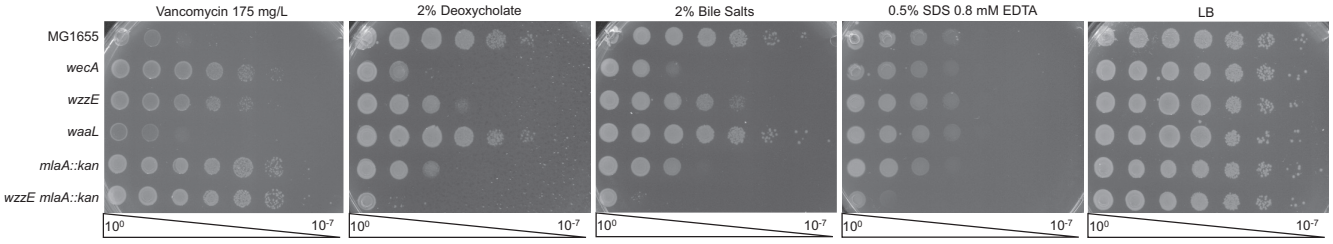

FIG 6 ECA_{CYC} plays a role in maintaining the OM permeability barrier. To assay changes to the OM due to removal of ECA_{CYC}, EOPs were performed on strains with the indicated deletions. Removing ECA_{CYC} is responsible for some of the changes to the OM permeability barrier caused by ECA deletions. Combining *wzzE* and *mlaA* deletions caused synthetic SDS EDTA sensitivity. Images are representative of three independent experiments.

lanes 4 and 5): (i) the amount of ECA_{LPS} and ECA_{PG} is increased; (ii) more short (less than 6 copies) and long (more than 7 copies) ECA chains are made; (iii) no ECA_{CYC} is produced (see Fig. S7). Given that completely removing ECA suppresses the Δ*yhdP* strain's phenotypes and *yhdP* deletion increases levels of ECA_{LPS} and ECA_{PG}, we find it unlikely that the mechanism through which *wzzE* deletion suppresses the Δ*yhdP* strain's phenotypes is through further increasing these levels. To investigate the possibility that increasing or decreasing ECA chain length suppresses the Δ*yhdP* strain, we tested the Δ*yhdP* strain's envelope permeability and suppression at 30°C, where the modal chain length of ECA appears to be four copies; at 37°C the modal chain length of ECA is six to seven copies (Fig. 5B). Although intrinsic sensitivities to SDS EDTA and vancomycin differ between these temperatures, neither temperature suppresses the Δ*yhdP* strain's phenotypes, nor does the suppression of the Δ*yhdP* strain occur by preventing ECA synthesis change. Thus, despite the fact that *yhdP* deletion lowered ECA_{CYC} levels, preventing ECA_{CYC} synthesis suppressed the envelope permeability of Δ*yhdP* strains, demonstrating a specific, functional interaction between YhdP and ECA_{CYC}.

ECA_{CYC} maintains the OM permeability barrier. As the presence of ECA_{CYC} leads to damage to the OM permeability barrier in the absence of YhdP, we then asked whether, in wild-type cells, ECA_{CYC} plays a broader role in maintaining the OM permeability barrier. With high-throughput studies, the specificity of effects caused by insertions in the *wec* operon can be unclear, as these mutations, including those in *wzzE*, can be polar, causing loss of all ECA species (28). Thus, we investigated changes to envelope permeability with clean *wzzE* deletion.

Cells with Δ*wzzE* showed a level of vancomycin resistance that was higher than that in *wzzE*$^+$ cells and was, in fact, equal to that of Δ*wecA* cells (Fig. 6). The vancomycin resistance was similar to that observed with deletion of *mlaA*. MlaA is the first protein in the Mla pathway, which facilitates retrograde phospholipid transport and is responsible for preventing phospholipids from accumulating in the outer leaflet of the OM (59). In addition to vancomycin resistance, Δ*wzzE* cells also show sensitivity to deoxycholate, a detergent derived from bile salts, although less than that observed in Δ*wecA* cells. Deletion of *waaL*, which prevents formation of ECA_{LPS}, had no effect on vancomycin resistance or DOC sensitivity. As WaaL does not influence deoxycholate resistance, these data suggest that both ECA_{PG} and ECA_{CYC} contribute to the deoxycholate phenotype, while ECA_{CYC} is responsible for vancomycin phenotype. Interestingly, combining strain Δ*wzzE* and *mlaA* deletion leads to an increase in SDS EDTA, deoxycholate, and bile salt sensitivity over that observed with either parent strain. This increase in detergent sensitivity suggests that combining these deletions causes larger changes to the OM than result from the individual mutations. Overall, these data demonstrate removal of ECA_{CYC} causes clear changes to the OM permeability barrier.

DISCUSSION

In this work, we have established that ECA_{CYC} helps to maintain the OM permeability barrier and that YhdP controls this activity of ECA_{CYC} in such a way as to prevent damage to the OM. ECA_{CYC}, not the membrane-associated form of ECA, is responsible

for some of the OM permeability phenotypes caused by removal of ECA. Furthermore, in a Δ*yhdP* background, uncontrolled aberrant activity of ECA_{CYC} causes envelope permeability despite the fact that removing YhdP greatly lowered levels of ECA_{CYC}. This role in maintenance of the OM permeability barrier is the first phenotype described for ECA_{CYC}.

ECA is conserved throughout *Enterobacteriaceae* despite one of the OM forms acting as a surface-exposed common antigen that can lead to antibody production (29). Therefore, ECA must perform cellular functions that justify not only the risk of expressing a common antigen but also the potential for damage caused by ECA_{CYC}. For the surface-exposed forms of ECA, one can imagine roles relating to direct host interactions, such as receptor binding interactions, interactions with other members of *Enterobacteriaceae*, or roles directly influencing the penetration of toxic substances into the cell; however, it is very difficult to imagine that ECA_{CYC}, from its location in the periplasm, is responsible for interacting with the environment. Instead, ECA_{CYC} must play a role intrinsic to the cell. The changes in OM permeability that occur with removal of ECA_{CYC} demonstrate that ECA_{CYC} plays a role in maintaining the barrier function of the OM.

ECA_{CYC}, as a cyclic soluble molecule made of aminosugars, has some resemblance to cyclodextrins. Cyclodextrins are cyclic carbohydrates made of glucose monomers that have a hydrophilic exterior and a hydrophobic cavity that allows them to bind to hydrophobic guests to increase their solubility and decrease their volubility (60). In fact, some cyclodextrins can pull specific molecules, such as cholesterol, out of membranes without binding to or disrupting the membranes (61–63). These properties have led to their use in drug formulations, as food additives, in cosmetics, as air deodorizers, and in many other applications (64). It is tempting to speculate that ECA_{CYC} may have similar properties allowing it to bind to specific target molecules in the periplasm and transfer them to or from the OM. In this case, it may be that YhdP is responsible for controlling what molecules are bound or where and how the molecules are unloaded.

Despite the large size of YhdP and strong phenotypes caused by its removal (36, 38), it is not apparent that YhdP has any unique role independent of ECA_{CYC}, emphasizing the importance to the cell of controlling ECA_{CYC} activity. This also makes YhdP an important tool allowing for investigation of the effects of uncontrolled ECA_{CYC} in order to elucidate its normal function. The decrease in ECA_{CYC} in the Δ*yhdP* strain likely reflects a cellular mechanism to decrease the OM damage due to ECA_{CYC} in the absence of YhdP. The cell compensates for the loss of YhdP either through decreased synthesis or increased degradation of ECA_{CYC} to minimize OM damage. It is also possible that some ECA_{CYC} may leak out of Δ*yhdP* cells due to the OM damage; however, the methods for detecting ECA_{CYC} make this very difficult to determine. Nevertheless, even the low levels of ECA_{CYC} remaining are capable of damaging the OM barrier when its activity is uncontrolled. In the future, it will be of interest to investigate the mechanisms through which ECA levels are regulated. Nevertheless, our data suggest that, in the absence of ECA_{CYC} downregulation, the phenotypes of the Δ*yhdP* strain would be extremely severe.

Although the structure and topology of YhdP have not been experimentally determined, it is predicted to be an inner membrane protein with an N-terminal and possibly a C-terminal transmembrane helix, with the remainder of the protein exposed in the periplasm (37). YhdP is classified as a member of the AsmA family of proteins due to the presence of a C-terminal AsmA_2 domain and an N-terminal DUF3971 domain, which contain shared sequence motifs with those found in AsmA (58). In *E. coli*, there are six members of this family, AsmA, YhdP, TamB (YtfN), YhjG, YicH, and YdbH (65). Although the function of these proteins is largely unknown, mutations in *asmA* have been found to suppress assembly-defective mutations in OMPs (66, 67). In addition, TamB has been suggested to interact with the OMP TamA to allow secretion of autotransporters (68). Half of the DUF490 domain of TamA has been crystallized and found to adopt a "taco-shaped" β-sheet with a hydrophobic cavity (69). The remainder of the protein is thought to adopt a similar conformation, perhaps allowing amphipathic OMP segments

to be transferred to TamA to avoid the aqueous periplasm. This structure is similar to that of the β-jellyroll conformation found in the LptA protein responsible for LPS transport across the periplasm (69, 70).

Although TamA and YhdP share only 25% identity, it is possible that YhdP adopts a similar conformation allowing it to bind to hydrophobic molecules. If this is the case, then YhdP may bind to hydrophobic molecules and pass them to ECA_{CYC} or unload molecules from ECA_{CYC}. We are currently investigating the specific mechanisms and pathways through which YhdP and ECA_{CYC} act, including the possibility that YhdP and ECA_{CYC} may interact physically. Nevertheless, the functional interaction between YhdP and ECA_{CYC} and the strong phenotype caused by ECA_{CYC} in the absence of YhdP represent an important aspect to envelope biology that has yet to be explored.

The difference in cellular location between ECA_{CYC} and the other forms of ECA, the ability of the cell to make three forms of ECA, and the differing antibiotic sensitivities with removal between these forms, suggests that the function of ECA_{CYC} and YhdP are likely not the same as the functions of ECA_{PG} and ECA_{LPS}. In addition, while ECA_{PG} has a role, direct or indirect, in excluding toxic substances, ECA_{LPS} appears to have no role in maintaining the OM permeability barrier and may instead have a role in interacting with the environment or be a by-product of the reaction that attaches O antigen to LPS. Interestingly, when investigating changes to the various forms of ECA in the presence and absence of *yhdP*, we observed that the modal chain length of the membrane-bound forms of ECA varied based on temperature. Knowledge on changes in ECA chain length in response to temperature has not been reported. This change in chain length may be due to specific regulation of ECA length by temperature or by a temperature-dependent change in the activity of the ECA polymerase, WzyE. However, in *Yersinia enterocolitica*, expression of ECA has been found to be modulated by temperature changes, with high levels of ECA at 22°C and almost undetectable levels at 37°C (71, 72). These data suggest that the functional requirements for the membrane-bound forms of ECA may depend on temperature. Furthermore, the differences in regulation of ECA expression between genera in *Enterobacteriaceae* suggest that the role of ECA may be adapted or modified for the lifestyles of different species. Investigation of these differences may lead to interesting insights into the biology of these species.

MATERIALS AND METHODS

Strains and growth conditions. The strains used in this work are listed in Table S2. Cultures were grown at 37°C in LB medium unless otherwise noted. When necessary, cultures were supplemented with 20 mg/liter chloramphenicol, 25 mg/liter kanamycin, or 25 mg/liter tetracycline. To quantitate ECA_{CYC} levels, cells were grown in M63 medium without nitrogen and supplemented with 0.2% glucose, 0.2% $(NH_4)_2SO_4$, 1 mM $MgSO_4$, and 100 μg/ml thiamine. Deletion alleles originated from the Keio collection (73), unless otherwise noted, and were moved into our strains by P1*vir* transduction (74). Unless otherwise indicated, resistance cassettes were flipped out as has been described previously (75).

Antibiotic sensitivity assays. For growth curves, overnight cultures were diluted 1:1,000 into 2 ml fresh LB containing the compounds indicated in a 24-well format, sealed with breathable film, and grown shaking at 37°C in a BioTek Synergy H1 plate reader. The optical density at 600 nm (OD_{600}) was assayed every 10 min. MICs were determined as has been reported elsewhere (57). The MIC was taken to be the minimum concentration of antibiotic at which no growth was observed. For efficiency of plating (EOP) assay, 10-fold dilutions of overnight cultures were made and replicate plated onto LB plates supplemented with the indicated chemicals. Plates were incubated at 30°C (unless otherwise noted) overnight and plates were imaged.

Generation and mapping of suppressor mutations. To generate spontaneous suppressor mutants, we plated 10^7 Δ*yhdP* strain cells on LB supplemented with 70 mg/liter vancomycin and incubated the plates overnight at 30°C. Colonies were picked and subjected to secondary screening for vancomycin and SDS EDTA resistance. The suppressor mutations were mapped as has been described elsewhere (76). We generated a Tn*5* mutant library in a Δ*yhdP* strain as has been described elsewhere (36). Our selection and screening strategy for isolating suppressing mutations is outlined in Fig. S3A. The transposon insertion site were determined by arbitrary PCR as has been described previously (59), except that the TetA-out and TetA-seq primers were replaced with Tn5-out (5′ GGTTGTAACACTGGCAGAGC 3′) and Tn5-seq (5′ TCCGTGGCAAAGCAAAAGTT 3′).

Phylogenetic co-occurrence and homologies. To determine whether *yhdP* and the genes of the *wec* operon tend to occur in the same genomes across organisms, we utilized the co-occurrence channel of STRING-DB (39, 77). We searched the database in multiple-protein mode for *yhdP* and ECA biosynthesis genes and took the phylogenetic co-occurrence scores from the generated table. The derivation of these scores from homology tables has been described elsewhere (77). To examine the level of homology for

possible YhdP homologues, we used the homology scores generated via the STRING database to find whether the indicated classification of organisms was predicted to have an YhdP homology and what the highest and lowest homology scores were for the organisms included in STRING-DB within that classification. These scores were then plotted.

σ^E reporter assay. To determine the level of activation of the σ^E system, we utilized a plasmid reporter with the promoter from *micA* driving expression of GFP (57) as has been reported elsewhere (78). Each of the three independent experiments was conducted in technical triplicate. The significance of the differences observed was calculated using the nonparametric Mann-Whitney test.

Quantification of ECA levels. Membrane-associated forms of ECA were analyzed by immunoblot analysis. Cells from an overnight culture were resuspended in BugBuster protein extraction reagent (Millipore Sigma) at an equivalent OD_{600} of 40 and then combined with an equal volume of Laemmli sample buffer (Bio-Rad) with 4% β-mercaptoethanol. Samples were boiled 5 min and then cooled and loaded on 12% TGX gels (Bio-Rad). The samples were transferred to nitrocellulose and were probed with a 1:10,000 dilution of anti-ECA antibody. Rabbit polyclonal anti-ECA antibody was a kind gift from Renato Morona (University of Adelaide). Donkey anti-rabbit secondary antibody conjugated to horseradish peroxidase was utilized at a 1:20,000 dilution and detected using a Crescendo ECL system (Millipore Sigma). The specificity of the ECA antibody could be observed based on the lack of signal with the Δ*wecA* strain (Fig. 4B, lanes 1 and 6). Levels of ECA were quantitated using ImageJ. Densitometry was performed on blots with the lowest exposure at which the ECA bands for the indicated samples could be detected. Densitometry was performed on the whole lane and manually baselined. Similar results were found when each ECA band was measured individually. For each of three to five biological replicates, fold values to the *yhdP*$^+$ sample were calculated. Then, the biological replicates were averaged and the standard errors of the means (SEM) were calculated. Significance was calculated using the Mann-Whitney test.

ECA_{CYC} was purified as has been described before, with minor modifications (34). Cells were grown in LB medium for determination of the ECA_{CYC} structure. For determination of ECA_{CYC} levels, cells were grown in M63 medium with either a normal or heavy (^{15}N) nitrogen source, and cultures for comparison were combined at the beginning of purification. After ethanol precipitation, supernatants were lyophilized and subsequently resuspended with 0.1% formic acid. Acidified samples were loaded on C_{18} StageTips (79), washed twice with 0.1% formic acid, and eluted with 20% acetonitrile with 0.1% formic acid. Eluates were then dried in a Speedvac before reconstitution with 20% acetonitrile. Samples were analyzed by MALDI-TOF/mass spectroscopy as has been previously described (34). Spectra were obtained with a Bruker UltrafleXtreme instrument calibrated with Red phosphorous. For relative quantification, the ratio of the areas of the heavy and normal ECA_{CYC} peaks was calculated for three biological replicates. Significance was calculated using the Mann-Whitney test.

SUPPLEMENTAL MATERIAL

Supplemental material for this article may be found at https://doi.org/10.1128/mBio.01321-18.

FIG S1, EPS file, 2.7 MB.
FIG S2, EPS file, 1.1 MB.
FIG S3, EPS file, 1.3 MB.
FIG S4, JPG file, 0.3 MB.
FIG S5, EPS file, 1.7 MB.
FIG S6, EPS file, 1.8 MB.
FIG S7, EPS file, 2.5 MB.
FIG S8, JPG file, 0.3 MB.
TABLE S1, DOCX file, 0.01 MB.
TABLE S2, DOCX file, 0.03 MB.

ACKNOWLEDGMENTS

We thank the current and previous members of the Silhavy laboratory for productive discussions. We thank Renato Morona (University of Adelaide) for the kind gift of anti-ECA antibody. We also thank Henry Shwe from the Princeton Department of Molecular Biology proteomics and mass spectrometry core for preparation of ECA_{CYC} samples.

This work was funded by the National Institute of General Medical Sciences grant GM118024 and fellowship F32GM116188.

REFERENCES

1. Silhavy TJ, Kahne D, Walker S. 2010. The bacterial cell envelope. Cold Spring Harb Perspect Biol 2:a000414. https://doi.org/10.1101/cshperspect.a000414.
2. Raetz CR, Whitfield C. 2002. Lipopolysaccharide endotoxins. Annu Rev Biochem 71:635–700. https://doi.org/10.1146/annurev.biochem.71.110601.135414.
3. Nikaido H. 2003. Molecular basis of bacterial outer membrane permea-

bility revisited. Microbiol Mol Biol Rev 67:593–656. https://doi.org/10.1128/MMBR.67.4.593-656.2003.
4. Kuhn H, Meier-Dieter U, Mayer H. 1988. ECA, the enterobacterial common antigen. FEMS Microbiol Lett 54:195–222. https://doi.org/10.1111/j.1574-6968.1988.tb02743.x.
5. World Health Organization. 2014. Antimicrobial resistance: global report on surveillance. WHO, Geneva, Switzerland.
6. Kunin CM. 1963. Separation, characterization, and biological significance of a common antigen in *Enterobacteriaceae*. J Exp Med 118:565–586. https://doi.org/10.1084/jem.118.4.565.
7. Rick PD, Hubbard GL, Barr K. 1994. Role of the *rfe* gene in the synthesis of the O8 antigen in *Escherichia coli* K-12. J Bacteriol 176:2877–2884. https://doi.org/10.1128/jb.176.10.2877-2884.1994.
8. Klena JD, Schnaitman CA. 1993. Function of the *rfb* gene cluster and the *rfe* gene in the synthesis of O antigen by *Shigella dysenteriae*. Mol Microbiol 9:393–402. https://doi.org/10.1111/j.1365-2958.1993.tb01700.x.
9. Alexander DC, Valvano MA. 1994. Role of the rfe gene in the biosynthesis of the *Escherichia coli* O7-specific lipopolysaccharide and other O-specific polysaccharides containing N-acetylglucosamine. J Bacteriol 176:7079–7084. https://doi.org/10.1128/jb.176.22.7079-7084.1994.
10. Danese PN, Oliver GR, Barr K, Bowman GD, Rick PD, Silhavy TJ. 1998. Accumulation of the enterobacterial common antigen lipid II biosynthetic intermediate stimulates *degP* transcription in *Escherichia coli*. J Bacteriol 180:5875–5884.
11. Jorgenson MA, Kannan S, Laubacher ME, Young KD. 2016. Dead-end intermediates in the enterobacterial common antigen pathway induce morphological defects in *Escherichia coli* by competing for undecaprenyl phosphate. Mol Microbiol 100:1–14. https://doi.org/10.1111/mmi.13284.
12. Castelli ME, Véscovi EG. 2011. The Rcs signal transduction pathway is triggered by enterobacterial common antigen structure alterations in *Serratia marcescens*. J Bacteriol 193:63–74. https://doi.org/10.1128/JB.00839-10.
13. Klein KA, Fukuto HS, Pelletier M, Romanov G, Grabenstein JP, Palmer LE, Ernst R, Bliska JB. 2012. A transposon site hybridization screen identifies *galU* and *wecBC* as important for survival of *Yersinia pestis* in murine macrophages. J Bacteriol 194:653–662. https://doi.org/10.1128/JB.06237-11.
14. Phan MD, Peters KM, Sarkar S, Lukowski SW, Allsopp LP, Gomes Moriel DG, Achard MES, Totsika M, Marshall VM, Upton M, Beatson SA, Schembri MA. 2013. The serum resistome of a globally disseminated multidrug resistant uropathogenic *Escherichia coli* clone. PLoS Genet 9:e1003834. https://doi.org/10.1371/journal.pgen.1003834.
15. Suezawa C, Yasuda M, Negayama K, Kameyama T, Hirauchi M, Nakai T, Okuda J. 2016. Identification of genes associated with the penetration activity of the human type of *Edwardsiella tarda* EdwGII through human colon epithelial cell monolayers. Microb Pathog 95:148–156. https://doi.org/10.1016/j.micpath.2016.04.007.
16. Bohm K, Porwollik S, Chu W, Dover JA, Gilcrease EB, Casjens SR, McClelland M, Parent KN. 2018. Genes affecting progression of bacteriophage P22 infection in Salmonella identified by transposon and single gene deletion screens. Mol Microbiol 108:288–305. https://doi.org/10.1111/mmi.13936.
17. Barua S, Yamashino T, Hasegawa T, Yokoyama K, Torii K, Ohta M. 2002. Involvement of surface polysaccharides in the organic acid resistance of Shiga toxin-producing Escherichia coli O157:H7. Mol Microbiol 43:629–640. https://doi.org/10.1046/j.1365-2958.2002.02768.x.
18. Ramos-Morales F, Prieto AI, Beuzón CR, Holden DW, Casadesús J. 2003. Role for Salmonella enterica enterobacterial common antigen in bile resistance and virulence. J Bacteriol 185:5328–5332. https://doi.org/10.1128/JB.185.17.5328-5332.2003.
19. Gilbreath JJ, Colvocoresses Dodds J, Rick PD, Soloski MJ, Merrell DS, Metcalf ES. 2012. Enterobacterial common antigen mutants of *Salmonella enterica* serovar Typhimurium establish a persistent infection and provide protection against subsequent lethal challenge. Infect Immun 80:441–450. https://doi.org/10.1128/IAI.05559-11.
20. Lugowski C, Romanowska E, Kenne L, Lindberg B. 1983. Identification of a trisaccharide repeating-unit in the enterobacterial common-antigen. Carbohydr Res 118:173–181. https://doi.org/10.1016/0008-6215(83)88045-8.
21. Männel D, Mayer H. 1978. Isolation and chemical characterization of the enterobacterial common antigen. Eur J Biochem 86:361–370. https://doi.org/10.1111/j.1432-1033.1978.tb12318.x.
22. Rick PD, Mayer H, Neumeyer BA, Wolski S, Bitter-Suermann D. 1985. Biosynthesis of enterobacterial common antigen. J Bacteriol 162:494–503.
23. Barr K, Nunes-Edwards P, Rick PD. 1989. In vitro synthesis of a lipid-linked trisaccharide involved in synthesis of enterobacterial common antigen. J Bacteriol 171:1326–1332. https://doi.org/10.1128/jb.171.3.1326-1332.1989.
24. Rick P, Silver R. 1996. Enterobacterial common antigen and capsular polysaccharides, p 104–122. *In* Neidhardt FC, Curtiss R, III, Ingraham JL, Lin ECC, Low KB, Magasanik B, Reznikoff WS, Riley M, Schaechter M, Umbarger HE (ed), *Escherichia coli* and *Salmonella*: cellular and molecular biology, 2nd ed. ASM Press, Washington, DC.
25. Rahman A, Barr K, Rick PD. 2001. Identification of the structural gene for the TDP-Fuc4NAc:lipid II Fuc4NAc transferase involved in synthesis of enterobacterial common antigen in *Escherichia coli* K-12. J Bacteriol 183:6509–6516. https://doi.org/10.1128/JB.183.22.6509-6516.2001.
26. Rick PD, Barr K, Sankaran K, Kajimura J, Rush JS, Waechter CJ. 2003. Evidence that the *wzxE* gene of *Escherichia coli* K-12 encodes a protein involved in the transbilayer movement of a trisaccharide-lipid intermediate in the assembly of enterobacterial common antigen. J Biol Chem 278:16534–16542. https://doi.org/10.1074/jbc.M301750200.
27. Brade H. 1999. Endotoxin in health and disease. CRC Press, Boca Raton, FL.
28. Barr K, Klena J, Rick PD. 1999. The modality of enterobacterial common antigen polysaccharide chain lengths is regulated by o349 of the *wec* gene cluster of *Escherichia coli* K-12. J Bacteriol 181:6564–6568.
29. Schmidt G, Mannel D, Mayer H, Whang HY, Neter E. 1976. Role of a lipopolysaccharide gene for immunogenicity of the enterobacterial common antigen. J Bacteriol 126:579–586.
30. Kuhn HM, Neter E, Mayer H. 1983. Modification of the lipid moiety of the enterobacterial common antigen by the "Pseudomonas factor." Infect Immun 40:696–700.
31. Rinno J, Golecki JR, Mayer H. 1980. Localization of enterobacterial common antigen: immunogenic and nonimmunogenic enterobacterial common antigen-containing *Escherichia coli*. J Bacteriol 141:814–821.
32. Acker G, Bitter-Suermann D, Meier-Dieter U, Peters H, Mayer H. 1986. Immunocytochemical localization of enterobacterial common antigen in *Escherichia coli* and *Yersinia enterocolitica* cells. J Bacteriol 168:348–356. https://doi.org/10.1128/jb.168.1.348-356.1986.
33. Erbel PJA, Barr K, Gao N, Gerwig GJ, Rick PD, Gardner KH. 2003. Identification and biosynthesis of cyclic enterobacterial common antigen in *Escherichia coli*. J Bacteriol 185:1995–2004. https://doi.org/10.1128/JB.185.6.1995-2004.2003.
34. Kajimura J, Rahman A, Rick PD. 2005. Assembly of cyclic enterobacterial common antigen in *Escherichia coli* K-12. J Bacteriol 187:6917–6927. https://doi.org/10.1128/JB.187.20.6917-6927.2005.
35. Dell A, Oates J, Lugowski C, Romanowska E, Kenne L, Lindberg B. 1984. The enterobacterial common-antigen, a cyclic polysaccharide. Carbohydr Res 133:95–104. https://doi.org/10.1016/0008-6215(84)85186-1.
36. Mitchell AM, Wang W, Silhavy TJ. 2017. Novel RpoS-dependent mechanisms strengthen the envelope permeability barrier during stationary phase. J Bacteriol 199:e00708-16. https://doi.org/10.1128/JB.00708-16.
37. Krogh A, Larsson Br, von Heijne G, Sonnhammer ELL. 2001. Predicting transmembrane protein topology with a hidden Markov model: application to complete genomes1. J Mol Biol 305:567–580. https://doi.org/10.1006/jmbi.2000.4315.
38. Nichols RJ, Sen S, Choo YJ, Beltrao P, Zietek M, Chaba R, Lee S, Kazmierczak KM, Lee KJ, Wong A, Shales M, Lovett S, Winkler ME, Krogan NJ, Typas A, Gross CA. 2011. Phenotypic landscape of a bacterial cell. Cell 144:143–156. https://doi.org/10.1016/j.cell.2010.11.052.
39. Szklarczyk D, Morris JH, Cook H, Kuhn M, Wyder S, Simonovic M, Santos A, Doncheva NT, Roth A, Bork P, Jensen LJ, von Mering C. 2017. The STRING database in 2017: quality-controlled protein-protein association networks, made broadly accessible. Nucleic Acids Res 45:D362–D368. https://doi.org/10.1093/nar/gkw937.
40. Nikaido H, Vaara M. 1985. Molecular basis of bacterial outer membrane permeability. Microbiol Rev 49:1–32.
41. Pootoolal J, Neu J, Wright GD. 2002. Glycopeptide antibiotic resistance. Annu Rev Pharmacol Toxicol 42:381–408. https://doi.org/10.1146/annurev.pharmtox.42.091601.142813.
42. Nikaido H. 2005. Restoring permeability barrier function to outer membrane. Chem Biol 12:507–509. https://doi.org/10.1016/j.chembiol.2005.05.001.
43. Sklar JG, Wu T, Gronenberg LS, Malinverni JC, Kahne D, Silhavy TJ. 2007. Lipoprotein SmpA is a component of the YaeT complex that assembles outer membrane proteins in Escherichia coli. Proc Natl Acad Sci U S A 104:6400–6405. https://doi.org/10.1073/pnas.0701579104.
44. Ricci DP, Hagan CL, Kahne D, Silhavy TJ. 2012. Activation of the Esche-

richia coli beta-barrel assembly machine (Bam) is required for essential components to interact properly with substrate. Proc Natl Acad Sci U S A 109:3487–3491. https://doi.org/10.1073/pnas.1201362109.
45. Rigel NW, Schwalm J, Ricci DP, Silhavy TJ. 2012. BamE modulates the Escherichia coli beta-barrel assembly machine component BamA. J Bacteriol 194:1002–1008. https://doi.org/10.1128/JB.06426-11.
46. Meier-Dieter U, Barr K, Starman R, Hatch L, Rick PD. 1992. Nucleotide sequence of the *Escherichia coli rfe* gene involved in the synthesis of enterobacterial common antigen. Molecular cloning of the *rfe-rff* gene cluster. J Biol Chem 267:746–753.
47. Marolda CL, Valvano MA. 1995. Genetic analysis of the dTDP-rhamnose biosynthesis region of the *Escherichia coli* VW187 (O7:K1) *rfb* gene cluster: identification of functional homologs of *rfbB* and *rfbA* in the *rff* cluster and correct location of the *rffE* gene. J Bacteriol 177:5539–5546. https://doi.org/10.1128/jb.177.19.5539-5546.1995.
48. Grabowicz M, Andres D, Lebar MD, Malojčić G, Kahne D, Silhavy TJ. 2014. A mutant Escherichia coli that attaches peptidoglycan to lipopolysaccharide and displays cell wall on its surface. eLife 3:e05334. https://doi.org/10.7554/eLife.05334.
49. Tamaki S, Nakajima S, Matsuhashi M. 1977. Thermosensitive mutation in Escherichia coli simultaneously causing defects in penicillin-binding protein-1Bs and in enzyme activity for peptidoglycan synthesis in vitro. Proc Natl Acad Sci U S A 74:5472–5476. https://doi.org/10.1073/pnas.74.12.5472.
50. Marquardt JL, Siegele DA, Kolter R, Walsh CT. 1992. Cloning and sequencing of Escherichia coli murZ and purification of its product, a UDP-N-acetylglucosamine enolpyruvyl transferase. J Bacteriol 174:5748–5752. https://doi.org/10.1128/jb.174.17.5748-5752.1992.
51. Apfel CM, Takács B, Fountoulakis M, Stieger M, Keck W. 1999. Use of genomics to identify bacterial undecaprenyl pyrophosphate synthetase: cloning, expression, and characterization of the essential uppS gene. J Bacteriol 181:483–492.
52. Paradis-Bleau C, Kritikos G, Orlova K, Typas A, Bernhardt TG. 2014. A genome-wide screen for bacterial envelope biogenesis mutants identifies a novel factor involved in cell wall precursor metabolism. PLoS Genet 10:e1004056. https://doi.org/10.1371/journal.pgen.1004056.
53. El Ghachi M, Bouhss A, Blanot D, Mengin-Lecreulx D. 2004. The bacA gene of Escherichia coli encodes an undecaprenyl pyrophosphate phosphatase activity. J Biol Chem 279:30106–30113. https://doi.org/10.1074/jbc.M401701200.
54. Dong J, Iuchi S, Kwan HS, Lu Z, Lin EC. 1993. The deduced amino-acid sequence of the cloned cpxR gene suggests the protein is the cognate regulator for the membrane sensor, CpxA, in a two-component signal transduction system of Escherichia coli. Gene 136:227–230. https://doi.org/10.1016/0378-1119(93)90469-J.
55. Gottesman S, Trisler P, Torres-Cabassa A. 1985. Regulation of capsular polysaccharide synthesis in Escherichia coli K-12: characterization of three regulatory genes. J Bacteriol 162:1111–1119.
56. De Las Peñas A, Connolly L, Gross CA. 1997. σ^E is an essential sigma factor in Escherichia coli. J Bacteriol 179:6862–6864. https://doi.org/10.1128/jb.179.21.6862-6864.1997.
57. Konovalova A, Grabowicz M, Balibar CJ, Malinverni JC, Painter RE, Riley D, Mann PA, Wang H, Garlisi CG, Sherborne B, Rigel NW, Ricci DP, Black TA, Roemer T, Silhavy TJ, Walker SS. 2018. Inhibitor of intramembrane protease RseP blocks the σ^E response causing lethal accumulation of unfolded outer membrane proteins. Proc Natl Acad Sci U S A https://doi.org/10.1073/pnas.1806107115.
58. Finn RD, Bateman A, Clements J, Coggill P, Eberhardt RY, Eddy SR, Heger A, Hetherington K, Holm L, Mistry J, Sonnhammer ELL, Tate J, Punta M. 2014. Pfam: the protein families database. Nucleic Acids Res 42:D222–D230. https://doi.org/10.1093/nar/gkt1223.
59. Malinverni JC, Silhavy TJ. 2009. An ABC transport system that maintains lipid asymmetry in the Gram-negative outer membrane. Proc Natl Acad Sci U S A 106:8009–8014. https://doi.org/10.1073/pnas.0903229106.
60. Kfoury M, Landy D, Fourmentin S. 2018. Characterization of cyclodextrin/volatile inclusion complexes: a review. Molecules 23:1204. https://doi.org/10.3390/molecules23051204.
61. Ohtani Y, Irie T, Uekama K, Fukunaga K, Pitha J. 1989. Differential effects of alpha-, beta- and gamma-cyclodextrins on human erythrocytes. Eur J Biochem 186:17–22. https://doi.org/10.1111/j.1432-1033.1989.tb15171.x.
62. Klein U, Gimpl G, Fahrenholz F. 1995. Alteration of the myometrial plasma membrane cholesterol content with beta-cyclodextrin modulates the binding affinity of the oxytocin receptor. Biochemistry 34:13784–13793. https://doi.org/10.1021/bi00042a009.
63. Yancey PG, Rodrigueza WV, Kilsdonk EP, Stoudt GW, Johnson WJ, Phillips MC, Rothblat GH. 1996. Cellular cholesterol efflux mediated by cyclodextrins. Demonstration of kinetic pools and mechanism of efflux. J Biol Chem 271:16026–16034. https://doi.org/10.1074/jbc.271.27.16026.
64. Crini G. 2014. Review. A history of cyclodextrins. Chem Rev 114:10940–10975.
65. Heinz E, Selkrig J, Belousoff MJ, Lithgow T. 2015. Evolution of the translocation and assembly module (TAM). Genome Biol Evol 7:1628–1643. https://doi.org/10.1093/gbe/evv097.
66. Deng M, Misra R. 1996. Examination of AsmA and its effect on the assembly of *Escherichia coli* outer membrane proteins. Mol Microbiol 21:605–612. https://doi.org/10.1111/j.1365-2958.1996.tb02568.x.
67. Misra R, Miao Y. 1995. Molecular analysis of asmA, a locus identified as the suppressor of OmpF assembly mutants of *Escherichia coli* K-12. Mol Microbiol 16:779–788. https://doi.org/10.1111/j.1365-2958.1995.tb02439.x.
68. Selkrig J, Mosbahi K, Webb CT, Belousoff MJ, Perry AJ, Wells TJ, Morris F, Leyton DL, Totsika M, Phan M-D, Celik N, Kelly M, Oates C, Hartland EL, Robins-Browne RM, Ramarathinam SH, Purcell AW, Schembri MA, Strugnell RA, Henderson IR, Walker D, Lithgow T. 2012. Discovery of an archetypal protein transport system in bacterial outer membranes. Nat Struct Mol Biol 19:506–510. https://doi.org/10.1038/nsmb.2261.
69. Josts I, Stubenrauch CJ, Vadlamani G, Mosbahi K, Walker D, Lithgow T, Grinter R. 2017. The structure of a conserved domain of TamB reveals a hydrophobic β taco fold. Structure 25:1898–1906.e5. https://doi.org/10.1016/j.str.2017.10.002.
70. Bollati M, Villa R, Gourlay LJ, Benedet M, Dehò G, Polissi A, Barbiroli A, Martorana AM, Sperandeo P, Bolognesi M, Nardini M. 2015. Crystal structure of LptH, the periplasmic component of the lipopolysaccharide transport machinery from Pseudomonas aeruginosa. FEBS J 282:1980–1997. https://doi.org/10.1111/febs.13254.
71. Muszyński A, Rabsztyn K, Knapska K, Duda KA, Duda-Grychtoł K, Kasperkiewicz K, Radziejewska-Lebrecht J, Holst O, Skurnik M. 2013. Enterobacterial common antigen and O-specific polysaccharide coexist in the lipopolysaccharide of Yersinia enterocolitica serotype O:3. Microbiology 159:1782–1793. https://doi.org/10.1099/mic.0.066662-0.
72. Rabsztyn K, Kasperkiewicz K, Duda KA, Li CM, Lukasik M, Radziejewska-Lebrecht J, Skurnik M. 2011. Characterization of anti-ECA antibodies in rabbit antiserum against rough Yersinia enterocolitica O:3. Biochemistry 76:832–839. https://doi.org/10.1134/S0006297911070145.
73. Baba T, Ara T, Hasegawa M, Takai Y, Okumura Y, Baba M, Datsenko KA, Tomita M, Wanner BL, Mori H. 2006. Construction of *Escherichia coli* K-12 in-frame, single-gene knockout mutants: the Keio collection. Mol Syst Biol 2:2006.0008. https://doi.org/10.1038/msb4100050.
74. Silhavy TJ, Berman ML, Enquist LW. 1984. Experiments with gene fusions. Cold Spring Harbor Laboratory Press, Cold Spring Harbor, NY.
75. Datsenko KA, Wanner BL. 2000. One-step inactivation of chromosomal genes in *Escherichia coli* K-12 using PCR products. Proc Natl Acad Sci U S A 97:6640–6645. https://doi.org/10.1073/pnas.120163297.
76. Button JE, Silhavy TJ, Ruiz N. 2007. A suppressor of cell death caused by the loss of σ^E downregulates extracytoplasmic stress responses and outer membrane vesicle production in Escherichia coli. J Bacteriol 189:1523–1530. https://doi.org/10.1128/JB.01534-06.
77. Franceschini A, Lin J, von Mering C, Jensen LJ. 2016. SVD-phy: improved prediction of protein functional associations through singular value decomposition of phylogenetic profiles. Bioinformatics 32:1085–1087. https://doi.org/10.1093/bioinformatics/btv696.
78. Konovalova A, Schwalm JA, Silhavy TJ. 2016. A suppressor mutation that creates a faster and more robust σ^E envelope stress response. J Bacteriol 198:2345–2351. https://doi.org/10.1128/JB.00340-16.
79. Rappsilber J, Mann M, Ishihama Y. 2007. Protocol for micro-purification, enrichment, pre-fractionation and storage of peptides for proteomics using StageTips. Nat Protoc 2:1896–1906. https://doi.org/10.1038/nprot.2007.261.